water

MDPI

Article

Adsorption Removal of Organophosphates from Water by Steel Slag: Modification, Performance, and Energy Site Analysis

Wei Wu [1], Yiming Nie [1], Zhixin Wang [1], Tianyin Huang [1,2], Xiaoyi Xu [1], Hanhan Liu [3], Peirong Li [4] and Bingdang Wu [1,2,*]

[1] School of Environmental Science and Engineering, Suzhou University of Science and Technology, Suzhou 215009, China; wuwei@usts.edu.cn (W.W.); nieyiming1998@163.com (Y.N.); koleratuer@163.com (Z.W.); huangtianyin111@163.com (T.H.); xuxiaoyiskd@usts.edu.cn (X.X.)
[2] Key Laboratory of Suzhou Sponge City Technology, Suzhou 215009, China
[3] Suzhou Chuanghailian Municipal Design Co., Suzhou 215000, China; sdhzzqz1998@163.com
[4] Suzhou Nadaqing Eco-Technology Co., Suzhou 215000, China; lprkycn@126.com
* Correspondence: wubingdang@usts.edu.cn

Abstract: Organophosphates are a type of emerging environmental contaminant, which can be removed effectively by adsorption. Here, modified steel slag was examined for its adsorptive performance in the removal of hydroxyethylidene diphosphonic acid (HEDP) from water. Compared to acid (55.3%, maximum removal rate) and base (85.5%) modification, high-temperature modification (90.6%) significantly enhanced steel slag's adsorption capacity for HEDP, surpassing that of unmodified slag (71.2%). Kinetic analyses elucidated a two-phase adsorption process—initial rapid adsorption followed by a slower equilibrium phase. The results of adsorption energy analysis showed that modified steel slag preferentially occupied the sites with higher energy, which promoted the adsorption. After five regeneration cycles, the adsorption properties of the material were not significantly reduced, which indicates that the material has good application potential. Microscopic and spectroscopic techniques, including SEM-EDS, FTIR, and XPS, were employed to uncover the surface chemistry and structural changes responsible for the enhanced adsorption efficiency. The adsorption mechanism of HEDP on steel slag is a complete process guided by hydrogen bonding interactions, strengthened surface complexation, and optimized ligand exchange. This study advances the sustainable utilization of industrial waste materials and contributes significantly to the development of innovative water treatment technologies.

Keywords: steel slag; organophosphates; adsorption; energy site; resource utilization

Citation: Wu, W.; Nie, Y.; Wang, Z.; Huang, T.; Xu, X.; Liu, H.; Li, P.; Wu, B. Adsorption Removal of Organophosphates from Water by Steel Slag: Modification, Performance, and Energy Site Analysis. *Water* **2024**, *16*, 3145. https://doi.org/10.3390/w16213145

Academic Editor: Yuanrong Zhu

Received: 11 September 2024
Revised: 24 October 2024
Accepted: 29 October 2024
Published: 3 November 2024

1. Introduction

Organophosphates are a class of pollutants that are widely present in the environment, and they are used as corrosion inhibitors, scale inhibitors, and chelating agents in a wide range of agricultural, industrial, and household cleaning products [1]. Among them, hydroxyethylidene diphosphonic acid (HEDP) is a common organophosphate that is widely used in the fields of water treatment, metal cleaning, and petroleum extraction due to its excellent chelating ability and its corrosion inhibition properties [2]. However, the excessive use and improper discharge of HEDP have led to water pollution problems, posing a potential threat to ecosystems and human health [3].

Presently, the predominant strategies for phosphate removal from aquatic environments encompass biological degradation, chemical precipitation, adsorption, and advanced oxidation techniques [4–8]. In some process, organophosphorus was broken down into inorganic byproducts such as phosphoric acid, nitric acid, ammonia, and formaldehyde, posing a significant risk for water body eutrophication. Therefore, adsorption has attracted much attention because of its simple operation and outstanding effect. Adsorption is accomplished by employing high-efficiency adsorbent materials, including activated carbon,

zeolites, metal oxides, and biochar, to sequester phosphate ions within the aqueous phase and immobilize them on the surfaces or within the porous structures of these materials [7]. Hence, there is a pressing demand for selecting the adsorbents with good adsorption effect, low price, and great practical application potential from many adsorption materials to address the challenge of organophosphorus pollutant treatment.

Steel slag, a byproduct of the iron and steel manufacturing sector, constitutes approximately 15% of crude steel production volume. Presently, the valorization of steel slag spans multiple domains, notably water treatment, soil amendment, construction material fabrication, and energy recovery [9]. Dom et al. pioneered a decentralized phosphorus removal system centered around steel slag filters, evaluating its efficacy, design parameters, and maintenance strategies [10]. Cha et al. reported on the near-total removal of phosphate during unsaturated soil aquifer treatment operations, demonstrating the efficacy of iron slag adsorption, albeit at low hydraulic loading rates [11]. In a novel approach, Wang et al. explored the feasibility of producing microbially mineralized steel slag bricks through a mineralization process to significantly enhance the strength of steel slag bricks, with an optimal SL/SS ratio of 0.3 for microbial mineralization. After a 3 h mineralization period post-demolding, the steel slag bricks exhibited a maximum compressive strength of 17.1 MPa and a flexural strength of 4.22 MPa [12]. Characterized by a rough surface and large specific surface area, steel slag exhibits advantageous properties for adsorption applications. Numerous studies have underscored steel slag's significant adsorption capacity for waterborne contaminants [13–16], encompassing phosphorus, heavy metal ions, and organic dyes. This underscores the environmental and economic significance of exploring steel slag's application as an adsorbent in water treatment processes. However, prior investigations into steel slag's efficacy in phosphorus removal have predominantly focused on inorganic phosphates, with scant attention directed towards organic phosphates [17].

Centering on hydroxyethylidene diphosphonic acid (HEDP), an organophosphate, as the focal subject of investigation, this study delves into the efficacy and underlying mechanisms of HEDP (Shanghai Aladdin Biochemical Technology Co., Ltd., Shanghai, China) adsorption onto steel slag. Characterization of the steel slag was carried out using an array of analytical techniques: scanning electron microscopy coupled with energy-dispersive X-ray spectroscopy (SEM-EDS), Fourier transform infrared spectroscopy (FTIR), and X-ray photoelectron spectroscopy (XPS, XRD). Kinetic and isotherm analyses were employed to elucidate the adsorption mechanism of HEDP by steel slag. This research endeavor intertwines the valorization of industrial waste with environmental pollution control, aiming to concurrently address waste management and solid waste resource utilization. Such an approach holds substantial promise for advancing ecological environmental protection and water treatment methodologies, underscoring its significant contributions to the field of environmental science and engineering.

2. Materials and Methods

2.1. Materials

The steel slag utilized in this investigation was sourced from Suzhou Nadaqing Company (Suzhou City, Jiangsu Province, China), with all materials subjected to thorough drying prior to experimentation to eliminate moisture and ensure the dryness and stability of the samples. The steel slag was mechanically milled and sieved through a 100-mesh sieve to achieve a homogenous particle size, optimizing its performance in adsorption processes. In alignment with stringent environmental and safety standards, this study conducted a comprehensive assessment of heavy metal leaching from the steel slag [18]. This assessment aimed to evaluate the potential environmental impact of steel slag in water treatment applications. The analytical scope encompassed the leaching levels of critical heavy metal elements, including iron, manganese, copper, zinc, cadmium, and lead. The results of the leaching test confirmed compliance with national standards, affirming the environmental safety of steel slag in water treatment contexts.

2.2. Modified Steel Slag Preparation

2.2.1. Acid-Modified Steel Slag

To prepare acid-modified steel slag (AS) samples at varying concentrations, the initial step involved precise weighing of the sieved steel slag, followed by its mixing with hydrochloric acid (Sinopharm Chemical Reagent Co., Ltd., Shanghai, China) of corresponding concentrations in a conical flask at a mass ratio of 1:100. In the literature, the concentration range used for acid modification is generally 0.1–3 mol/L [19]. In this study, in order to reflect the effect of corrosion caused by over-acid, the concentration range of 1–5 mol/L was chosen for this study. The resulting mixture was then subjected to a 24 h reaction period within a thermostatic oscillator, set at a temperature of 25 °C and a rotation speed of 150 rpm, ensuring thorough interaction between the acid and the steel slag. Upon completion of the reaction, the modified steel slag was isolated through filtration. Subsequent to this, the filtered material was placed in an oven at 105 °C for drying, a process aimed at completely eliminating any residual moisture. Post-drying, the AS underwent a second grinding and sieving process through a 100-mesh sieve to achieve a uniform particle size, ensuring consistency and readiness for subsequent experimental analyses.

2.2.2. Alkali-Modified Steel Slag

Adhering to a parallel methodology employed for acid modification, sodium hydroxide solution was substituted for hydrochloric acid to conduct the alkali modification (Sinopharm Chemical Reagent Co., Ltd., Shanghai, China) of steel slag, culminating in the acquisition of alkali-modified steel slag (ALS). The addition of alkali modifier also removed a large amount of calcium chloride and increased the specific surface area of steel slag; similarly, too much alkali destroys the pore structure of steel slag, so 1–5 mol/L sodium hydroxide solution was selected for the experiments [20]. The specific protocol encompassed the following stages: the precise weighing of steel slag was juxtaposed with that of sodium hydroxide solution, maintaining a mass ratio of 1:100. This mixture was then subjected to an identical oscillation regime as previously described, encompassing a temperature of 25 °C and a rotational speed of 150 rpm, for a duration of 24 h. Post-reaction, the ALS was isolated through filtration. Subsequently, it underwent a drying process in an oven at 105 °C to eradicate residual moisture. The final stage involved the steel slag's re-grinding and sieving through a 100-mesh sieve, ensuring a uniform particle size, thereby yielding a sample of ALS that was primed for experimental analysis.

2.2.3. Thermally Modified Steel Slag

A precise quantity of the sieved steel slag was collected and meticulously placed within a porcelain crucible, which was then transferred into a muffle furnace. The steel slag underwent thermal activation at varying temperature settings, each maintained for a duration of one hour to ensure uniform thermal treatment. Upon completion of the activation process, the high-temperature-modified steel slag (HTS) was subjected to a re-grinding procedure to achieve a consistent particle size. This was followed by a sieving step through a 100-mesh sieve to ensure the homogeneity of the particle size distribution. The culmination of this sequence resulted in the collection of samples of HES, categorized by different temperature gradients, ready for incorporation into subsequent experimental analyses.

2.3. Performance of Adsorbed HEDP

2.3.1. HEDP Adsorption Effect of Different Modified Steel Slags

Precisely 0.1 g of steel slag, modified through various techniques, was carefully placed into a 250 mL conical flask. Subsequently, 100 mL of phosphorus-containing wastewater, with a mass concentration of 10 mg/L (prepared using a 60% concentration of HEDP solution), was added to the flask. The mixtures were then subjected to a reaction period of 6 h at a constant temperature of 25 °C, with the oscillation rate maintained at 150 r/min, to ensure thorough interaction between the steel slag and the wastewater. Upon

the conclusion of the reaction, the supernatant was meticulously filtered through a 0.45 μm filter membrane. The phosphorus concentration within the filtered supernatant was then quantified. To ensure the robustness and reliability of the data, each sample underwent three replicates of the described process. By comparing the adsorption performance of steel slags modified by different methods on HEDP, the modified steel slag exhibiting the highest removal efficiency was identified and selected as the optimal adsorbent. The adsorption capacity (Q_e) and the removal rate (R) were calculated utilizing the following equations:

$$Q_e = \frac{(C_0 - C_e)V}{m} \quad (1)$$

$$R = \frac{(C_0 - C_e)}{C_0} \times 100\% \quad (2)$$

where Q_e is the amount of adsorbed phosphorus at equilibrium (mg/g), V is the volume of the solution (L), m is the mass of steel slag (g), and C_0 and C_e are the initial and equilibrium concentrations of phosphorus (mg/L), respectively.

2.3.2. Adsorption Kinetics Experiments

Exactly 0.1 g of steel slag was introduced into 100 mL of simulated wastewater, characterized by a phosphorus mass concentration of 10 mg/L. The mixture was then subjected to continuous agitation in a shaker at a controlled temperature of 25 °C, with the oscillation rate set at 150 r/min. At predetermined time intervals, 10 mL aliquots of the water samples were carefully withdrawn and filtered through a 0.45 μm filter membrane (BKMAMLAB Biotechnology Co., Ltd., Changde City, Hunan Province, China). The purpose of this filtration was to ascertain the residual phosphorus mass concentration in the filtrate. Utilizing the collected data, the quantity of phosphorus adsorbed, denoted as Q_t (mg/g), at distinct time points was calculated through the application of the following equation:

$$Q_t = \frac{V(C_0 - C_t)}{m} \quad (3)$$

where Q_t is the adsorption amount at time t (mg/g); C_0 is the initial mass concentration of phosphorus in the solution before adsorption (mg/L); C_t is the concentration of phosphorus in the supernatant after adsorption and filtration at time t (mg/L); V is the volume of the simulated water sample (L); and m is the amount of steel slag dosed (g).

The adsorption data were fitted to the kinetic model using Origin software 2022. The kinetic nature of the adsorption process was analyzed using pseudo-first order (4), pseudo-second order (5), and intra-particle diffusion (6) models:

$$\mathrm{In}(Q_e - Q_t) = \ln Q_e - k_1 T \quad (4)$$

$$\frac{t}{Q_t} = \frac{1}{k_2 Q_e^2} + \frac{t}{Q_e} \quad (5)$$

$$Q_t = K_{pi} t^{0.5} + C_i \quad (6)$$

where Q_e is the P adsorption of steel slag at equilibrium time (mg/g) and Q_t is the adsorption at time t (mg/g); k_1 and k_2 are the adsorption rate constants for the first/second order kinetic model ($g/mg{\cdot}h^{-1}$), respectively; and t is the adsorption time (h). K_{pi} ($mg/(g{\cdot}h^{0.5})$) is the rate constant of intra-particle diffusion; C_i is the intercept, which indicates the influence of the boundary layer thickness.

2.3.3. Adsorption Isotherms Experiments

First, 0.1 g of steel slag powder was added to 100 mL of simulated wastewater with phosphorus mass concentrations of 2 mg/L, 4 mg/L, 8 mg/L, 10 mg/L, 20 mg/L, 30 mg/L, 40 mg/L, 50 mg/L, 60 mg/L. The constant temperature was kept at 25 °C in the shaking table, and the water sample was taken as a 10 mL sample after continuous

shaking at a speed of 150 r/min for 24 h. The mass concentration of residual phosphorus was determined after the sample was passed through a 0.45 μm filter membrane. Then the model was fitted with the Langmuir and Freundlich isothermal adsorption models:

$$Q_e = \frac{Q_m k_L C_e}{1 + k_L C_e} \tag{7}$$

$$Q_e = k_f C_e^{\frac{1}{n}} \tag{8}$$

where K_L and K_f are Langmuir and Freundlich adsorption constants, respectively; n is a dimensionless coefficient; and Q_m is the theoretical maximum adsorption amount (mg/g).

2.3.4. Site Energy Distribution

The energy site distribution can visually describe the energy change in adsorption sites on the adsorbent surface. Based on the equations of the Langmuir model (7) and Freundlich model (8), the distribution of adsorption sites can be obtained according to the following Equations (9)–(11)

$$C_e = C_s \exp\left(-\frac{E - E_s}{RT}\right) = C_s \exp\left(-\frac{E^*}{RT}\right) \tag{9}$$

$$F(E^*) = \frac{Q_m K_L C_s}{RT} \exp\left(-\frac{E^*}{RT}\right)\left[1 + K_L C_s \exp\left(-\frac{E^*}{RT}\right)\right]^{-2} \tag{10}$$

$$F(E^*) = \frac{K_F C_s^n n}{RT} \exp\left(-\frac{nE^*}{RT}\right) \tag{11}$$

where $F(E^*)$ is the energy distribution function of the adsorption site (mg·mol·(kg·kJ^{-1})); C_s is the maximum solubility of the solute (mg/L); R is the gas constant, 8.314×10^{-3} kJ·mol^{-1}·K^{-1}; T is the absolute temperature (K); E is the adsorption energy at the concentration C_e (kJ/mol); E_s is the adsorption energy at the concentration C_s (kJ/mol); E^* is the adsorption energy difference between solute and solvent on the surface of the adsorbent based on the reference point E_s.

2.3.5. Impact of pH

In our investigation into the adsorption of HEDP by steel slag, it became apparent that environmental factors, notably pH, could exert a substantial influence on the adsorption efficacy. With this insight, a series of experiments were meticulously designed to scrutinize the impact of pH on the adsorption performance of the optimally modified steel slag for HEDP. The experimental setup involved a 200 mL conical flask, into which 0.1 g of the optimally modified steel slag was added, alongside 10 mL of phosphorus-laden wastewater, characterized by a mass concentration of 10 mg/L. A critical step in these experiments was the precise adjustment of the solution's pH across a spectrum from 3 to 11, achieved through the judicious addition of an acid or base. The remainder of the experimental procedure mirrored the previously detailed steps, entailing continuous oscillation at a constant temperature of 25 °C and an oscillation rate of 150 r/min, until the adsorption process reached completion. Subsequent filtration through a 0.45 μm filter membrane was followed by the quantification of phosphorus concentration in the filtrate supernatant. Through comparative analysis of the adsorption efficiency of steel slag on HEDP under varying pH conditions, we aimed to gain a more nuanced understanding of how pH influences the adsorption dynamics, thereby providing a scientific foundation for the optimization of adsorption conditions.

2.3.6. Regeneration Experiment

In the adsorption process of steel slag for phosphorus removal, the adsorption capacity of the modified steel slag diminishes over time until it reaches saturation, whereupon the

adsorbent loses its ability to adsorb phosphorus. To address this limitation and ensure the reusability of the adsorbent, it is imperative to explore and evaluate the regeneration methods of the adsorbent to assess its recycling potential. Commonly employed regeneration techniques encompass microwave regeneration [21], vacuum resolution, solvent regeneration [22], and heating regeneration [23]. The hydroxyl group in sodium hydroxide can replace HEDP adsorbed on the surface of steel slag. In our experimental setup, we employed 100 mg of the adsorbent in a 100 mL solution of 10 mg/L HEDP, with the experimental conditions set at a temperature of 25 °C and an oscillation rate of 150 rpm for a period of 24 h. Upon the conclusion of the adsorption phase, the adsorbent was sequentially washed three times with alternating ethanol and deionized water, followed by freeze-drying of the steel slag. Subsequent experiments, termed secondary cycling experiments, were conducted using the recovered material, with further cycling experiments carried out in a similar manner. To effectively desorb phosphate from the adsorbent surface, we utilized a combination of NaOH and NaCl as a desorbent solution. This was achieved by adding 100 mL of a 6 M NaOH and 3 M NaCl solution to the reacted system and stirring for 1 h at 60 °C. Post-stirring, the phosphate and total phosphorus content in the solution were measured to evaluate the desorption efficacy. Through this series of experiments, we aimed to systematically assess the regeneration performance and recycling potential of steel slag as an adsorbent, providing a scientific foundation for its practical application.

2.3.7. Analytical Methods

In order to accurately determine the phosphorus concentration in HEDP, the concentration of HEDP was measured by liquid chromatography-mass spectrometry [24,25]. Total phosphorus (TP) was determined by the molybdenum blue spectrophotometric method [17]. The method first utilized a potassium persulfate digestion technique to effectively convert the HEDP in the sample to detectable orthophosphate. Next, orthophosphate reacted with ammonium molybdate and potassium antimony tartrate to form heteropolyacids, which were subsequently reduced by ascorbic acid to complexes with a characteristic blue color. The concentration of phosphorus in HEDP was obtained by precise measurement of the blue complex at 700 nm using a UV–visible spectrophotometer (UV-2450 Shimadzu, Japan).

In order to fully understand the interaction of steel slag on the HEDP solution, we have employed several advanced characterization methods. Firstly, by scanning electron microscopy (ZEISS Gemini SEM 360) coupled with the energy spectroscopy (EDS) technique, we carried out an in-depth study of the micro-morphology and elemental composition of the steel slag, which helped us to understand the physical structure and chemical composition of the slag. Secondly, the functional groups in the steel slag were analyzed using the Fourier Transform Infrared Spectroscopy (Thermo Fisher Scientific Nicolet iS20) technique, which revealed the chemical properties and possible reaction sites of the slag for us. To further understand the pore structure of the steel slag, we used mercury porosimetry to measure the pore size distribution of meso and macropores with a scanning range covering 5 nm to 500 μm, which helped us to understand the adsorption properties of the steel slag. Finally, through the X-ray photoelectron spectroscopy (Thermo Scientific K-Alpha, Rigaku SmartLab SE) technique, we deeply analyzed the elemental composition and valence states of the steel slag, which provided strong data support for a comprehensive understanding of its chemical properties and reaction mechanisms. Through these comprehensive analytical methods, we were not only able to accurately determine the concentration of phosphorus in HEDP, but also to comprehensively understand the nature of steel slag, which provides a scientific basis for optimizing the adsorption process and improving the adsorption efficiency and regeneration capacity.

3. Results and Discussion

3.1. Selection of Modification Methods

Figure 1 shows the experimental results of the removal rate of HEDP from steel slag treated with different modification methods. Taking the unmodified steel slag as a

control, we found that the removal rate of HEDP from steel slag modified by alkali and high-temperature calcination was significantly increased. Specifically, the removal rate of HEDP by unmodified steel slag was 71.20%, while the removal rates of HTS and ALS were as high as 90.56% and 85.50%, respectively, which were 19.36% and 14.30% higher than that of unmodified steel slag. On the contrary, the removal of HEDP by AS decreased to 55.30%, which was 15.90% lower than that of unmodified steel slag. This result indicates that high-temperature modification and alkali modification can significantly improve the adsorption performance of steel slag for HEDP, with high-temperature modification having the most significant effect. High temperature is conducive to the decomposition of the active component, thus producing finer transition metal oxides and facilitating the contact between the reactants and steel slag [26]. The role of sodium hydroxide in the modification process is to provide a certain alkalinity for the system. The higher the alkalinity of the steel slag, the greater its activity and, therefore, the greater the adsorption of HEDP. In summary, the HTS and ALS performed well in removing HEDP, especially the HTS, whose removal rate of HEDP was much higher than that of the other modified steel slags, which provided an effective solution for wastewater treatment. Meanwhile, the use of sodium hydroxide further enhanced the adsorption performance of the steel slag, which provided a new idea to optimize the adsorption effect of the modified steel slag. The ALS, examined by scanning electron microscopy (SEM), was found to have a rougher surface, with a significant increase in specific surface area and pore volume, which directly enhanced the physical adsorption capacity, resulting in a significantly higher phosphate removal rate from the modified steel slag than that from the unmodified steel slag [27]. This result indicates that alkali modification not only alters the physical properties of the slag, but also enhances its adsorption capacity for phosphate. In the acid modification process, the most intuitive change is that the color of the steel slag changes from brown to dark grey, which may be due to the fact that the metal oxides in the steel slag are dissolved in the form of metal cations during the acid modification process, thus reducing the adsorption performance of the steel slag for phosphate. The poor effect of acid modification may originate from the fact that the dissolution of metal oxides is not favorable to the adsorption and precipitation of phosphate under acidic conditions. At present, the effect of AS is still highly controversial, and the reason for the difference in results may be related to the fact that the physicochemical properties of the selected steel slag are themselves highly different. High-temperature calcination modification, especially at certain temperatures (e.g., 700 °C), can effectively remove the water and some impurities filling the interior of the steel slag without destroying the basic structure of the slag, thus releasing more space to improve the adsorption performance of the slag [28]. The experimental results showed that when the calcination temperature was lower than 800 °C, the adsorption performance of steel slag on HEDP in simulated wastewater increased gradually with the temperature, and the removal rate increased from 44.70% to 90.56%; however, as the temperature continued to increase, the removal rate began to decrease from 90.56% to 81.20%. At lower temperatures, the water molecules and impurities inside the steel slag structure are not sufficiently removed, and the enhancement of the adsorption performance is limited; whereas too high a temperature usually leads to the destruction of the steel slag structure, causing the pore size to collapse and the specific surface area to decrease, thus weakening the adsorption capacity. Taking the above experimental results into account, and considering the needs of subsequent experiments, we chose 700 °C as the optimal temperature for steel slag modification. The modified steel slag at this temperature not only has high adsorption performance, but also has good structural stability, and is suitable to be used as the adsorbent for subsequent experiments.

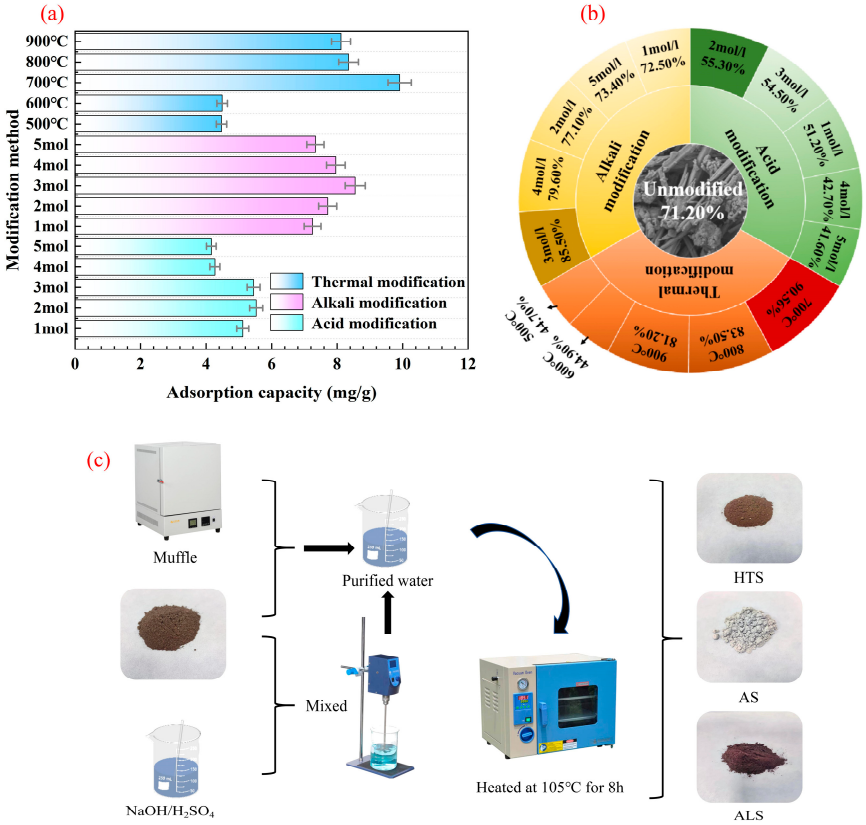

Figure 1. (**a**) Effect of different modification methods on the adsorption capacity of steel slag adsorption of HEDP, (**b**) Effect of modification methods on the adsorption of HEDP by steel slag, (**c**) Steel slag modification preparation process.

3.2. SEM, BET, and XRD Analyses

In order to deeply investigate the effect of high-temperature modification on the surface and pore structure of steel slag, we carried out detailed comparative analyses, including scanning electron microscope (SEM) images of steel slag before and after the modification and BET data analyses (Figure 2, Table 1). From the SEM images (Figure 2a,b), it can be clearly observed that the roughness of the steel slag surface increased significantly after the high-temperature modification, forming a rich multi-crack structure, which provided more active sites for adsorption. By BET analysis, we found that although the pore diameter decreased after high-temperature modification, the increase in total pore volume and specific surface area (Table 1) enhanced the density of adsorption sites, which was favorable for the adsorption of HEDP. As shown in Figure 2c,d, the N_2 adsorption isotherms conformed to the International Union of Pure and Applied Chemistry IUPAC type II characteristics, which indicated that the modification treatment had a significant effect on the pore structure of steel slag. As shown in Figure 2e,f, many spurious peaks are observed in the modified XRD spectra, indicating that the crystal phase composition of the steel slag is complex and poorly crystallized. After comparing with the standard XRD card, the main components found in the steel slag are dicalcium silicate, calcium carbonate, calcium iron oxide, and ferrous oxide. The oxygen in the silica–oxygen of the HTS was reduced and aggregated towards the iron oxide.

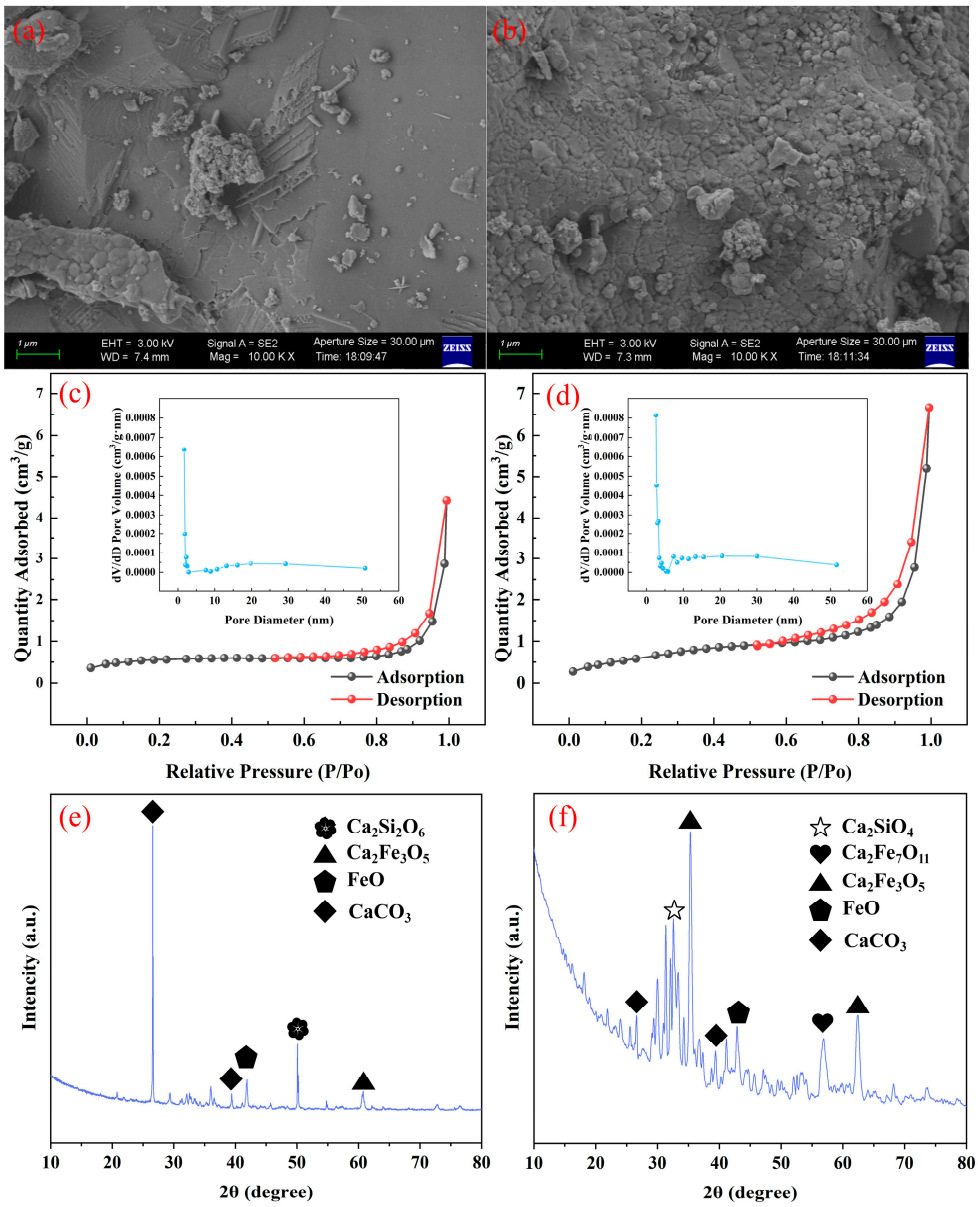

Figure 2. (**a**) SEM diagram of unmodified steel slag, (**b**) SEM diagram of HTS, (**c**) Specific surface area and pore volume aperture diagram of unmodified steel slag, (**d**) Specific surface area and pore volume aperture diagram of HTS, XRD images of steel slag before (**e**) and after (**f**) modification.

Table 1. BET analysis results before and after modification of steel slag.

Adsorbent	Specific Surface/($m^2 \cdot g^{-1}$)	Pore Volume/($cm^3 \cdot g^{-1}$)	Pore Size/(nm)
Unmodified steel slag	2.048	0.008994	19.6616
700 °C modified steel slag	2.3379	0.108621	15.5464

3.3. Adsorption Kinetics

Under the experimental conditions, i.e., dosage of 1.0 g/L, initial concentration of 10 mg/L, and temperature of 25 °C, we observed that the adsorption process reached equilibrium within 8 h (Figure 3a,b). The adsorption kinetic curves of both unmodified and HTS showed a similar trend: at the beginning of the adsorption process, i.e., within the first 30 min, the adsorption rate was very fast, which was mainly due to the abundance of active sites on the surface of the slag, which provided a large number of adsorption sites for the

HEDP [29]. However, the adsorption rate began to slow down gradually after 1 h, and at 8 h, the adsorption process basically reached equilibrium. Further extension of the adsorption time had little effect on the amount of phosphorus adsorbed, suggesting that the adsorption process is characterized by 'fast adsorption, slow equilibrium'. The fitting results of the kinetic model (Table 2) showed that both the pseudo-first order and pseudo-second order models can better describe the characteristics of HEDP adsorption from steel slag, and pseudo-first and pseudo-second order kinetics are often used to describe the adsorption of solutes by adsorbents. The pseudo-first order kinetic model assumes that adsorption is a single-step process and that the rate of adsorption is mainly limited by external diffusion, while the pseudo-second order kinetic model assumes that the adsorption process consists of multiple steps, such as external diffusion, internal diffusion, and chemical adsorption on the adsorption site, and that the rate of adsorption is controlled by the entire adsorption mechanism. However, the pseudo-first order model has the highest correlation coefficient, which indicates that the model is more in line with the experimental data. Before and after modification, the coefficients of the adsorption process reached 0.9949 and 0.9986, respectively, which indicated that the adsorption process followed the pseudo-first order kinetic law, i.e., the adsorption rate was mainly controlled by the active sites on the surface of the adsorbent [30]. The equilibrium adsorption quantities calculated by the pseudo-first order model were highly in agreement with the experimentally determined values with very little error, which further verified the applicability of the model in describing the kinetic process of adsorption and its accuracy. Under the set experimental conditions, the adsorption of HEDP from HTS was in accordance with the pseudo-first order kinetic model, showing fast adsorption and slow equilibrium.

Table 2. Pseudo-first order kinetics, pseudo-second order kinetics, and fitting parameters of intra granular diffusion of steel slag adsorption of HEDP before and after modification.

Kinetic Model	Adsorbent	Parameter	Result
The pseudo-first order	Unmodified steel slag	$Q_e/(mg \cdot g^{-1})$	7.1091
		k_1/min^{-1}	0.5547
		R^2	0.9949
	700 °C modified steel slag	$Q_e/(mg \cdot g^{-1})$	9.8893
		k_1/min^{-1}	0.5012
		R^2	0.9986
The pseudo-second order	Unmodified steel slag	$Q_e/(mg \cdot g^{-1})$	8.2616
		$k_2/(g \cdot mg^{-1} \cdot min^{-1})$	0.07841
		R^2	0.9701
	700 °C modified steel slag	$Q_e/(mg \cdot g^{-1})$	12.5881
		$k_2/(g \cdot mg^{-1} \cdot min^{-1})$	0.0495
		R^2	0.9917
Weber–Morris fitting	Unmodified steel slag	C_1	3.9205
		R^2	0.9963
		C_2	0.01701
		R^2	/
	700 °C modified steel slag	C_1	5.1569
		R^2	0.9957
		C_2	0.0512
		R^2	/

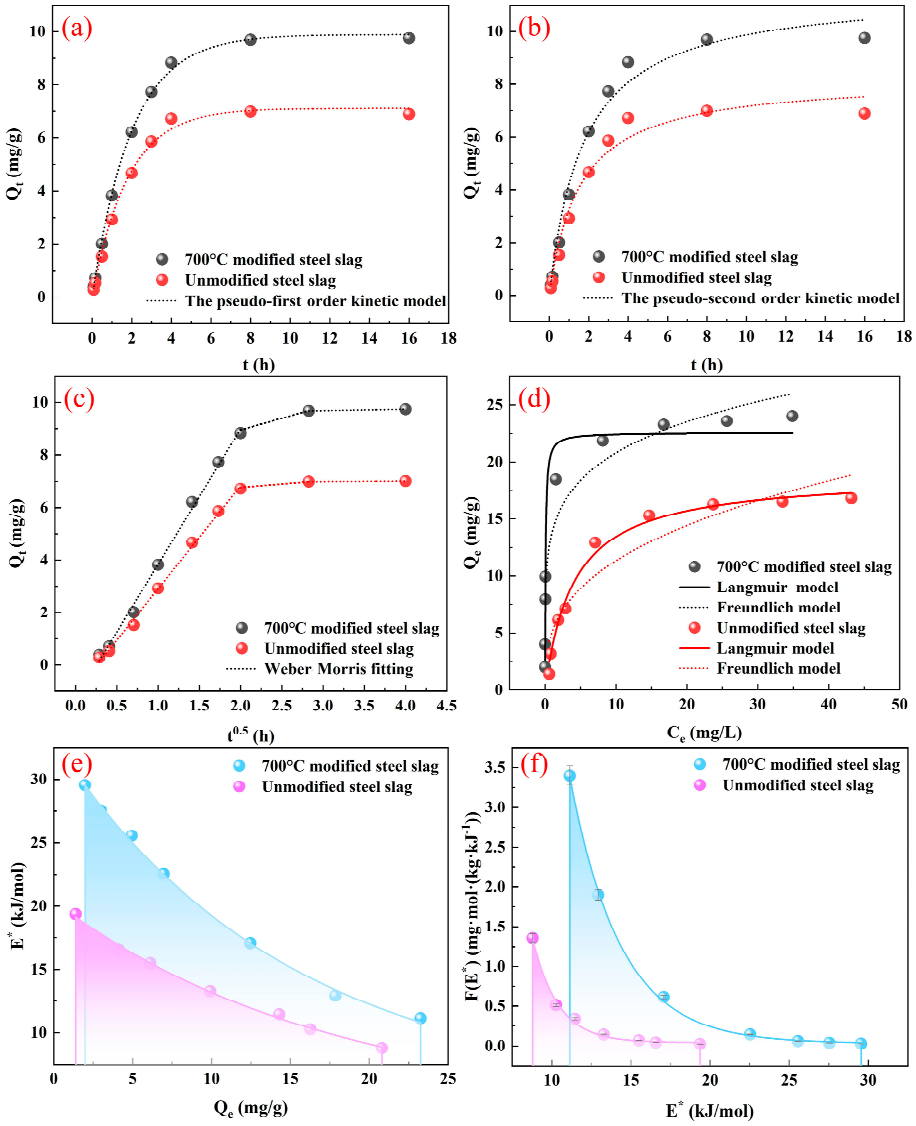

Figure 3. (**a**) Pseudo-first order kinetic fitting diagram of the adsorption of HEDP by steel slag before and after modification, (**b**) pseudo -second order kinetic fitting diagram of adsorption of HEDP by steel slag before and after modification, (**c**) Fitting diagram of intra granular diffusion of steel slag adsorbing HEDP before and after modification, (**d**) Quasi isotherm fitting diagram of adsorption of HEDP by steel slag before and after modification, (**e**) Relationship diagram between adsorption energy and adsorption capacity, (**f**) Site energy distribution based on adsorption isotherm model.

The fitting results of the intra-particle diffusion model (Figure 3c) revealed the complex nature of the adsorption kinetics, which was manifested as a two-stage process: the first stage was liquid film diffusion, in which HEDP diffused rapidly from the solution to the surface of the steel slag, at a faster diffusion rate; this was followed by a slower intra-particle diffusion stage, in which HEDP molecules diffused further through the internal pores of the steel slag, which was rate-limited, with the removal efficiency of organic phosphorus having a direct impact. From the morphology of the modeled curve, it does not show a single straight line across the origin, which suggests that the adsorption rate is governed by a combination of factors, including different adsorption mechanisms, chemical reaction rates, and diffusion factors. This observation is in agreement with the literature reports and further confirms the complexity of the HEDP adsorption process [31]. During the adsorption process, the mass transfer rate slowed down as the difference in HEDP concentration gradually decreased. At the same time, the number of active sites on the steel

slag surface gradually decreased as adsorption proceeded, which likewise slowed down the adsorption rate. When the adsorption and desorption rates reached equilibrium, the adsorption equilibrium state was reached. Therefore, both liquid film diffusion and intra-particle diffusion play key roles in the adsorption process of HEDP on steel slag, having a significant effect on the adsorption kinetics. The fitted parameters of the intra-particle diffusion model for the adsorption of HEDP on steel slag are listed in Table 2.

3.4. Adsorption Isotherms

From Figure 3d and Table 3, it can be seen that the adsorption isotherms fitted by the Langmuir and Freundlich models under the condition of 25 °C show that both models have high R^2 values. In the adsorption process of HEDP on steel slag before and after modification, the R^2 values of the Langmuir model were slightly higher than those of the Freundlich model, and the theoretical saturated adsorption capacity of 34.965 mg/g of HTS was introduced according to the model, which was increased by 58.32% compared with that of unmodified slag. As shown in Table 4, compared with other literatures, HTS has certain advantages in adsorption capacity The correlation coefficients of the Langmuir equations were more than 0.97, which indicated that the adsorption characteristics of steel slag on phosphate were consistent with the model. This kind of adsorption is mainly carried out by chemical precipitation and ligand exchange, which belongs to chemical adsorption [32]. Since the adsorption process on the solid surface in solution is a physicochemical process that includes heat absorption and an exothermic process, the value of K in the isothermal adsorption equation of Langmuir is a parameter related to the binding energy of the adsorption of solutes on the solid surface. Therefore, the magnitude of the K value indicates that the adsorption process of steel slag on HEDP in this paper is heat absorption, and the elevation of ambient temperature is conducive to the binding of HEDP to improve the purification efficiency. In the Freundlich model, the n value reflects the strength of adsorption, and the calculated 1/n values are all less than 1, which proves that HEDP can be adsorbed effectively by steel slag. Calcium oxide in the steel slag reacted with the HEDP solution to produce an amorphous calcium phosphate precipitate, and the isotherms maintained a large slope at high concentrations, which showed that the steel slag was well adapted to the changes in effluent concentration in the solid–liquid system and maintained an efficient treatment effect. This further confirms the great potential of steel slag as an organophosphate adsorbent.

Table 3. Langmuir and Freundlich equations fit adsorption isotherms.

Adsorbent	Langmuir Model			Freundlich Model		
	Q_m/(mg·g^{-1})	K_L/(L·mg^{-1})	R^2	K_F/(mg·g^{-1})	1/n	R^2
Unmodified steel slag	22.085	13.639	0.990	12.389	0.241	0.901
700 °C modified steel slag	34.965	0.083	0.973	3.311	0.510	0.929

Table 4. Comparison of Langmuir's theoretical maximum adsorption capacity of HEDP by different adsorbents.

Adsorbent	Q_m/(mg·g^{-1})	Reference
HTS	34.965	This study
Unmodified steel slag	22.085	This study
Eu-MOF/GO	37.31	[33]
Steel slag	23.74	[17]
Fe/La	16.58	
Fe/Eu	27.45	[34]
Fe/Ce	15.99	

3.5. Adsorption Site Energy

The area enclosed by the curve F(E*) and the x-axis represents the saturated adsorption of HEDP by the adsorbent, and the point E_m^* is the critical point that defines the energy distribution of the site. Points with adsorption energy less than E_m^* are known as low energy sites and vice versa for high energy sites. The public announcement is as follows:

$$E_m^* = RT(K_L C_s) \quad (12)$$

The energy distribution of the adsorption sites of steel slag in HEDP wastewater before and after modification is shown in Figure 3e,f. The energy distribution curve decreases with the increase in the E^* value, and still shows an "L" shape in the dicrystalline system. However, at the same concentration, the energy distribution of sites before and after modification is different. The site energy distribution of the modified slag is mainly concentrated in the range of 11.14–29.54 kJ/mol, with a site energy inhomogeneity of 6.73, while that of the pre-modified slag is in the range of 8.79–19.37 kJ/mol, with a site energy inhomogeneity of 3.48. The E_m^* of the modified steel slag surface is 24.61 kJ/mol, which is significantly larger than that of the unmodified steel slag surface of 11.96 kJ/mol. From the site energy inhomogeneity and isotherm analysis, it can be seen that the modified steel slag is biased towards inhomogeneous distribution, which indicates that the inhomogeneous distribution will increase the value of E_m^*, and the larger the value of E_m^*, the better the affinity between the adsorbent and adsorbate, which promotes the adsorption [35]. The results show that modified steel slag preferentially occupies the sites with higher energy, and the area under the distribution curve of the energy of the sites of the modified slag is much larger than the area under the distribution curve of the unmodified steel slag, due to the distribution curve of the unmodified steel slag. The area under the distribution curve can be regarded as the number of adsorption sites, which indicates that the modified steel slag occupies more adsorption sites than the pre-modified steel slag in the dual adsorption process. Therefore, the modified steel slag has an advantage in the adsorption capacity of HEDP.

3.6. Assessment of Practical Applications

3.6.1. Effect of pH

From Figure 4a,b, we can see that the equilibrium adsorption capacity of steel slag, both before and after modification, showed a trend of first increasing and then decreasing with the initial pH. In particular, the removal efficiency of HEDP by the HTS reached more than 95% in a weakly alkaline environment at pH 9, which indicated that the removal of HEDP by the steel slag was optimal under neutral to weakly alkaline conditions. This result is consistent with the negatively charged nature of the steel slag surface in alkaline solutions, as deprotonation by surface hydroxylation increases its negative charge, which enhances the adsorption of positively charged HEDP molecules. However, the removal efficiency of HEDP decreased slightly when the pH was increased to 11, which could be attributed to the increase in the negative charge of the steel slag surface at higher pH values, leading to electrostatic repulsion with the equally negatively charged organophosphates, thus reducing the adsorption efficiency. Nevertheless, considering that the removal rate of steel slag before and after modification remained relatively stable, we can speculate that electrostatic attraction is not the only or main factor determining the adsorption efficiency. In combination with Figure 4g,h, the large change in charge before and after adsorption indicates that surface electrostatic adsorption plays a large role. The surface metal of steel slag was positively charged, and after adsorption of organophosphorus as a site, the amount of positive charge decreased and showed more negative charge. And the potential of modified steel slag after adsorption of organophosphorus is lower compared to unmodified steel slag after adsorption, indicating that the high-temperature modification process exposes more metal ions on the surface of the material. The adsorption process showed relative insensitivity to changes in initial pH, which was mainly due to the buffering

capacity of steel slag. During the adsorption process, as the adsorption time increases, the dissolution of alkaline substances leads to an increase in the pH of the system, while the pH of the acidic solution increases accordingly. This pH change contributes to the enhanced phosphorus removal efficacy of steel slag, as a pH environment closer to neutrality reduces electrostatic repulsion and thus improves adsorption efficiency.

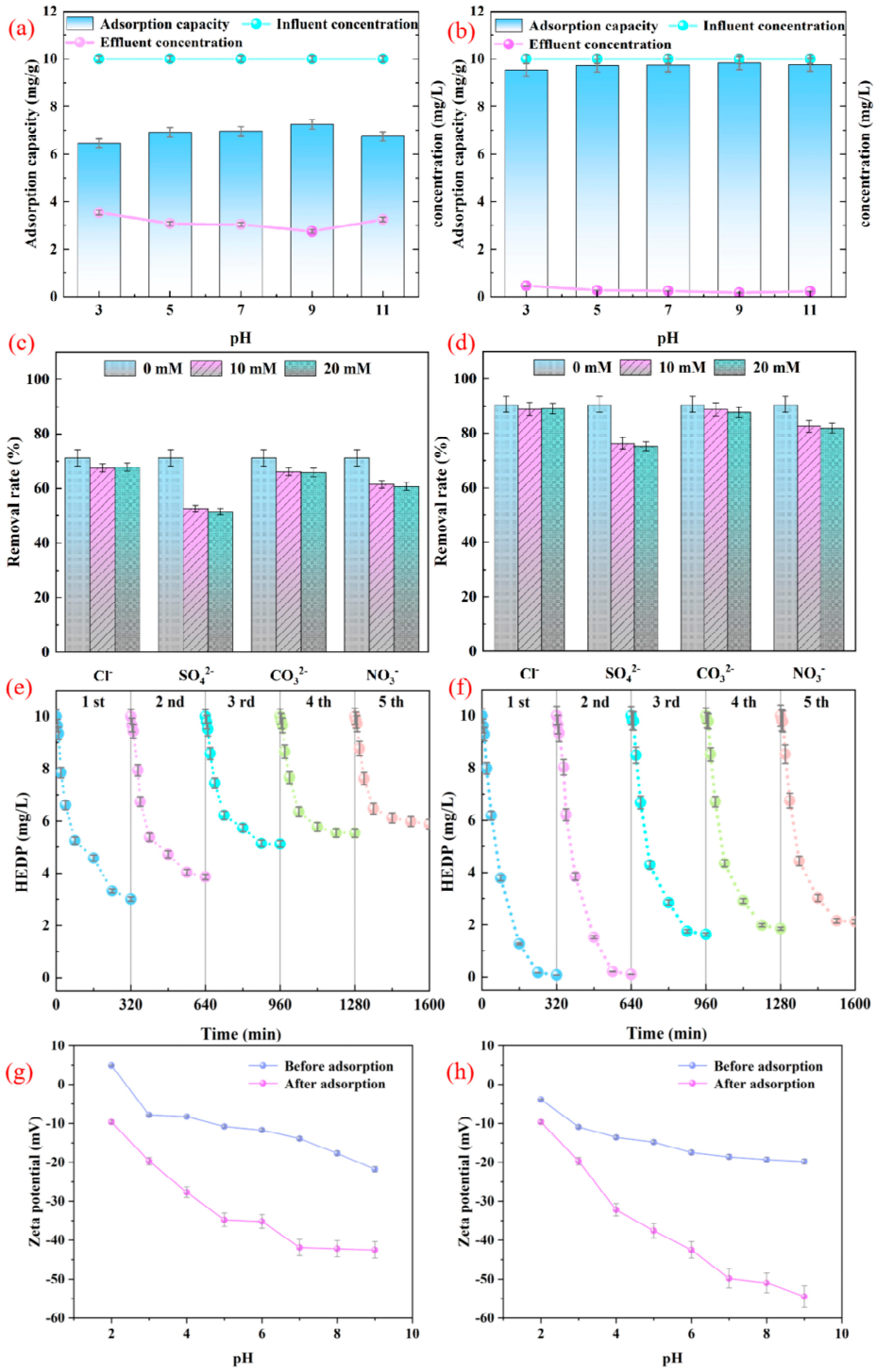

Figure 4. (**a**) Effect of pH on the removal of HEDP from unmodified steel slag, (**b**) Effect of pH on HEDP removal from HTS, (**c**) Effect of co-existing ions on the removal of HEDP from unmodified steel slag, (**d**) Effect of co-existing ions on HEDP removal by HTS, (**e**) Recycling of unmodified steel slag, (**f**) Recycling of HTS. Zeta potential diagrams before and after unmodified steel slag (**g**) and HTS (**h**) adsorption of HEDP.

3.6.2. Effect of Co-Existing Ions

Co-existing anions limited the adsorption capacity of the adsorbent for phosphate by occupying the adsorption sites and enhancing electrostatic repulsion. Figure 4c,d reveals that the adsorbent modified with high temperature mitigated the negative effect of anions on the adsorption process. Among them, chloride (Cl^-) and carbonate (CO_3^{2-}) ions had less effect on the adsorption of HEDP, which indicated that their competitive adsorption was weak [36]. In contrast, nitrate (NO_3^-) ions exerted a certain inhibitory effect on the adsorption of HEDP, which could be attributed to the existence of electrostatic repulsion between NO_3^- and HEDP as well as the negatively charged steel slag surfaces, which impeded the HEDP adsorption. Sulphate ions (SO_4^{2-}) exerted a more significant adverse effect on the adsorption process, which may be due to the fact that SO_4^{2-} binds to Ca^{2+}, resulting in the precipitation of almost or completely insoluble substances from the steel slag, which in turn reduces the active adsorption sites on the surface [37].

3.6.3. Adsorbent Regeneration

The data presented in Figure 4e,f clearly reveal a decreasing trend in the saturated adsorption capacity of the HTS during the desorption regeneration process. Specifically, the removal efficiency of modified steel slag for HEDP decreased from an initial level of about 98% to about 80% after five cycles. Notably, this efficiency level was significantly higher than the performance of unmodified steel slag, indicating that high-temperature modification enhanced the regeneration capacity and adsorption stability of steel slag to some extent. In the adsorption process, the chemisorption mechanism plays a dominant role. This means that the organophosphate molecules bound to the surface of the steel slag by chemical bonds are difficult to be completely removed by a simple alkaline washing process. These residual organophosphate molecules occupy active sites that would otherwise be available for the new adsorption process, which directly leads to a decrease in the adsorption efficiency. From the third to the fifth cycle, the removal efficiency stabilized at about 80% without significant fluctuations, indicating that the active sites on the surface of the steel slag had reached a new stable state after several adsorption–desorption cycles. The active adsorption sites on the surface of the steel slag were gradually saturated with the increase in the number of cycles, which meant that its initial adsorption capacity could not be fully recovered even by regeneration treatment [38]. This phenomenon led to the stabilization of the adsorption efficiency, which no longer decreased significantly with the increase in the number of cycles. Therefore, regarding the performance of HTS in the desorption and regeneration process, despite the decrease in adsorption efficiency, its stable regeneration capacity and superior performance over unmodified steel slag make it a promising and recyclable adsorbent in the field of wastewater treatment.

3.7. Adsorption Mechanism

By using the SEM-EDS technique to analyze the micro-morphology of HTS before and after adsorption of HEDP, we obtained abundant information. Figure 5a,c clearly demonstrate the significant changes on the surface of steel slag before and after adsorption. Before adsorption, the surface of steel slag showed slight concave–convex folds accompanied by irregular overlapping of massive particles, which reflected its original microstructural characteristics. However, after HEDP adsorption, the morphology of the steel slag surface changed significantly, forming densely arranged granular materials, which not only covered the original surface, but also clearly defined the boundaries with each other, and this change intuitively reflected the physical effects of the adsorption process on the surface of steel slag. In order to further reveal the differences in the material elements before and after adsorption, we carried out a detailed characterization using the EDS technique, and the resulting energy point-sweep spectra (Figure 5b,d) provided key evidence. It is obvious from the figure that the absorption peaks of phosphorus (P) were significantly enhanced and the mass percentage of elemental phosphorus increased from 0 to 2.54%, and this significant change directly proved that the steel slag successfully adsorbed a large amount

of phosphorus and effectively removed phosphorus from the solution, thus verifying its excellent phosphorus adsorption performance. In the EDS analysis after adsorption of HEDP, we also observed that the percentage of carbon (C), oxygen (O), silicon (Si), calcium (Ca), and other elements increased. The explanation for this phenomenon is closely related to the chemical composition of HEDP and its behavior during the adsorption process. HEDP contains the elements carbon and oxygen, and the adsorption process leads to the enrichment of these elements on the surface of the steel slag, which in turn increases the percentage of the elements C and O in the EDS assay. In addition, the silicate minerals contained in the steel slag may interact with organophosphorus compounds or participate in surface chemical reactions, leading to an increase in the proportion of Si elements in the EDS spectra. The reaction of elemental calcium with organophosphorus compounds formed complexes or precipitates, and this chemical process not only enhanced the proportion of elemental Ca in the detection, but also promoted the further enrichment of elemental C and O, thus explaining the effect of adsorption processes on the elemental composition of steel slag surfaces at the microscopic level.

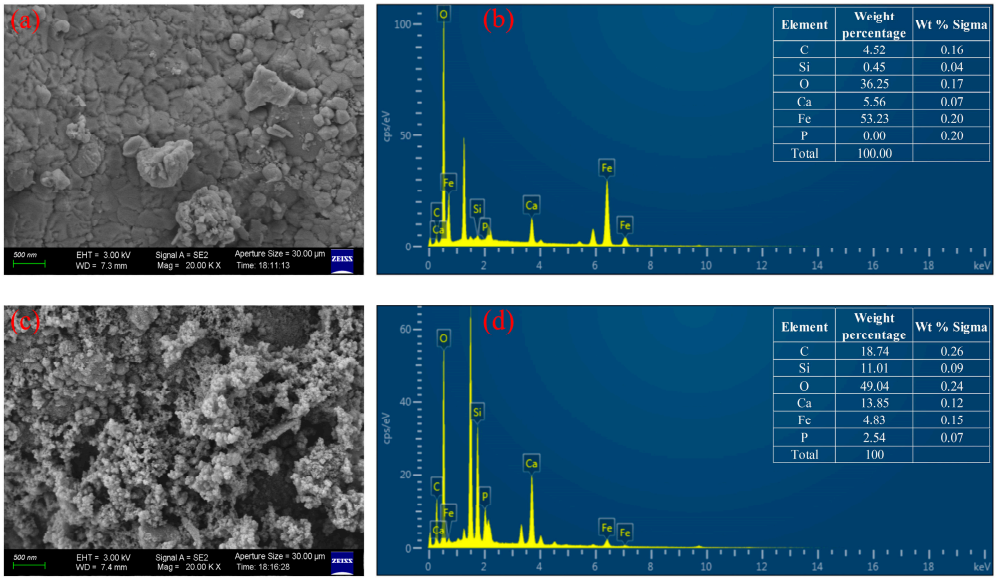

Figure 5. (**a**) SEM diagram of steel slag before adsorption, (**b**) EDS diagram of steel slag before adsorption, (**c**) SEM diagram of steel slag after adsorption, (**d**) EDS diagram of steel slag after adsorption.

Figure 6a shows slight changes in the stretching vibrational peaks corresponding to OH^- in the FTIR spectrograms, which are usually attributed to the enhancement of hydrogen bonding interactions between the HEDP molecules and hydroxyl groups on the surface of the steel slag or hydrated metal ions, as well as to desorption of water molecules that may take place during the adsorption process [39]. The hydroxyl groups of the HEDP molecules form hydrogen bonds with the hydroxyl groups on the surface of the steel slag, which enhances OH^- vibrational modes, leading to an increase in the intensity of the OH^- peak. The carbonate change at 1474 cm^{-1} indicates that the original carbonate ions on the steel slag surface have been replaced by HEDP molecules, i.e., a ligand exchange process has taken place. HEDP forms stronger complexes with metal ions on the steel slag surface, replacing the originally adsorbed carbonate ions, which leads to a weakening or disappearance of the intensity of the carbonate peak. In addition, a new absorption peak was observed at 1060 cm^{-1}, which is a characteristic peak of the phosphate group in the HEDP molecule, indicating that HEDP was successfully adsorbed on the surface of the steel slag. The appearance of the P-O peak confirms that the phosphate group in the HEDP molecule formed a stable chemical bond with the metal ions on the surface of the steel slag, i.e., the realization of the surface complexation process.

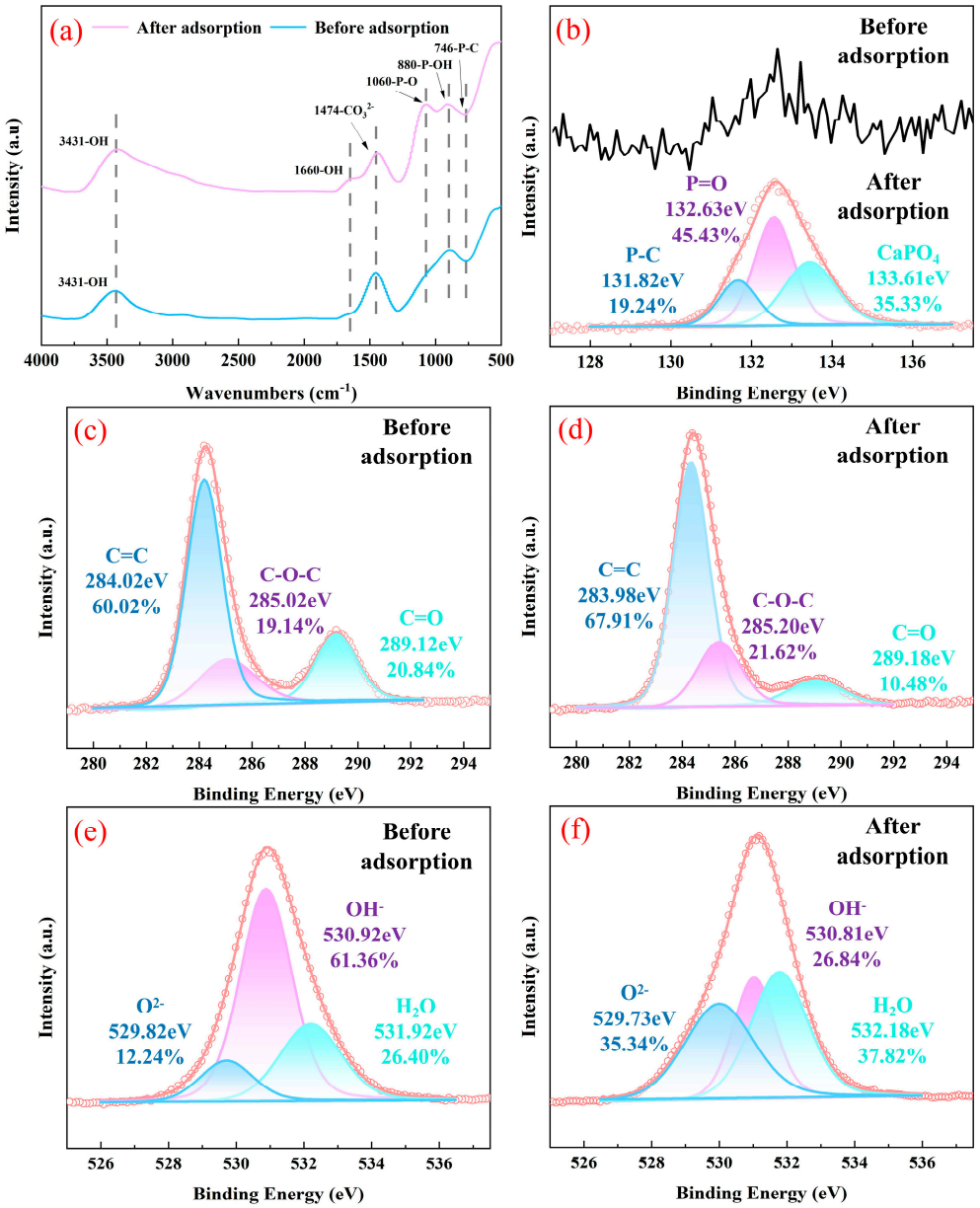

Figure 6. (**a**) Infrared spectra of steel slag before and after adsorption, (**b**) P2p spectra before and after steel slag adsorption of HEDP, C1s spectra before (**c**) and after (**d**) steel slag adsorption of HEDP, O1s spectra before (**e**) and after (**f**) steel slag adsorption of HEDP.

After XPS (Figure 6b–f) analysis, P peaks appeared after HEDP adsorption by steel slag, indicating the effectiveness of HEDP adsorption by steel slag, and both C1s and O1s spectra of steel slag adsorbed with HEDP were deconvoluted into three peaks. In the C1s spectra of Figure 6c,d, the peak located at 284.02 eV corresponds to saturated carbon (C–C), the peak at 285.02 eV corresponds to alcohols/ethers (C–O–C), and the peak at 289.12 eV corresponds to carboxyl carbonyls (C=O). Comparing with the XPS spectra before adsorption, the peak positions of saturated carbon and alcohol/ether shifted to higher binding energies after the adsorption of HEDP, which suggests that HEDP participates in the adsorption process as a new source of organic carbon, which enhances the signals of the C–C bond, and that the increase in the intensity of the signal of the alcohol/ether (C–O–C) may be attributed to the hydroxyl group (OH^-) in HEDP molecules forming hydroxyl groups with the surface of the steel slag during the adsorption process hydrogen bonds or other chemical interactions, thus enhancing the signals of C–O–C bonds and decreasing the signals of C=O bonds.

Meanwhile, in the O1s spectra of Figure 6e,f, the three peaks corresponded to O^{2-} (529.82 eV), OH^- (530.92 eV), and H_2O (532.18 eV), respectively. After adsorption of HEDP, the OH^- peak of steel slag was significantly reduced, which indicated that the HEDP molecules interacted with the hydroxyl structure on the surface of steel slag, probably through hydrogen bonding or coordination, leading to the reduction or transformation of the hydroxyl structure, which in turn reduced the intensity of the OH^- peak. Whereas, the elevation of O^{2-} (529.82 eV) and H_2O (532.18 eV) usually implies that the adsorption of HEDP molecules promotes the stabilization or formation of oxygen ions on the surface of the steel slag [40]. Phosphate groups in the HEDP molecules form complexes with metal ions on the surface of the steel slag, which promotes the stabilization of oxygen ions and the adsorption of water molecules [41]. The HEDP molecules are also known to form complexes with metal ions on the surface of the steel slag.

As shown in Figure 7, through the calculation, characterization, and analysis of the comprehensive adsorption test, and combined with the literature study, the adsorption mechanism of steel slag on HEDP can be summarized as follows:

1. Hydrogen bonding interactions: the hydroxyl and phosphate groups in the HEDP molecule are able to form hydrogen bonds with the hydroxyl or hydrated metal ions on the surface of steel slag. Although these hydrogen bonds are not covalent and their strength is relatively low, they play a crucial role in the positioning and stabilization of the molecules in the early stage of adsorption, which helps to promote the initial attachment of molecules.
2. Surface complexation: metal ions on the surface of steel slag, such as Fe and Ca, form stable complexes with the phosphate groups of HEDP through coordination. In this complexation process, the phosphate group acts as a ligand to provide lone-pair electrons to coordinate with the empty orbitals of the metal ions, thus building a strong chemical bond. This action significantly strengthens the adsorption strength, tunes the surface chemistry, and influences the subsequent adsorption behavior.
3. Ligand exchange: during the adsorption process, HEDP molecules can effectively replace the original ligands on the steel slag surface, such as water molecules and carbonate ions. As the complexes formed by HEDP and metal ions are more stable, it can adjust the surface chemical environment and optimize the adsorption conditions, thus significantly enhancing the adsorption efficiency.

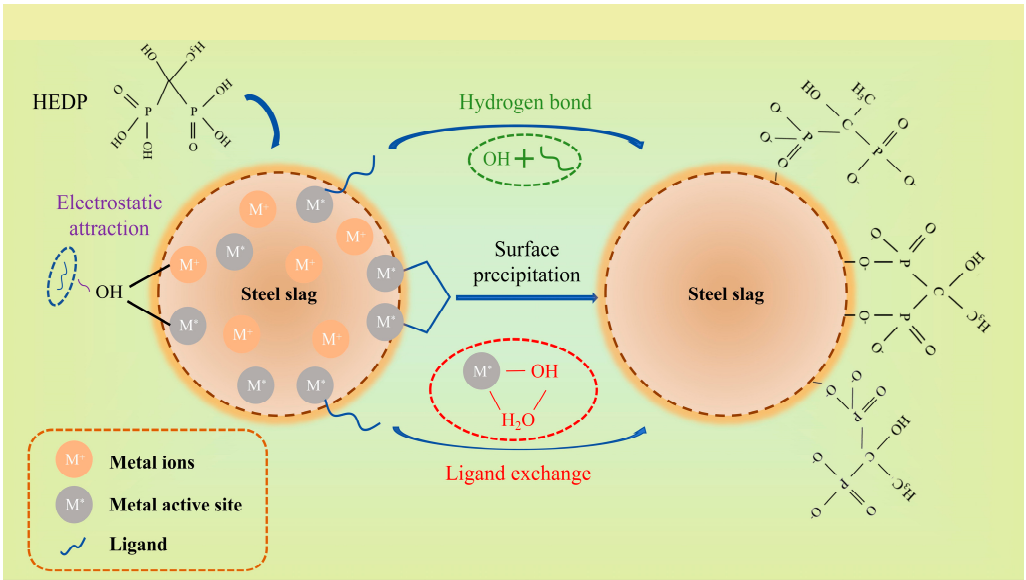

Figure 7. Diagram of the HEDP adsorption mechanism of steel slag.

In summary, the adsorption mechanism of HEDP on steel slag is a complete process guided by hydrogen bonding interactions, strengthened surface complexation, and optimized ligand exchange.

4. Conclusions

In this study, the efficacy and mechanism of adsorption of hydroxyethylidene diphosphate (HEDP) on HTS were investigated in depth, and the significant enhancement of the adsorption performance by the modification technology was revealed. The main findings are as follows:

1. Optimization of modification effect and conditions: High-temperature modification significantly enhanced the adsorption capacity of steel slag for HEDP, especially in the weak alkaline environment, and the removal efficiency of modified steel slag was up to more than 95%, which was significantly better than that of unmodified samples.
2. Adsorption kinetic analysis: The adsorption kinetics followed a quasi-one-stage model, indicating that the adsorption rate was controlled by the surface-active sites, and the adsorption process was divided into two phases: fast adsorption and slow equilibrium.
3. Adsorption mechanism and thermodynamics: The Langmuir model accurately described the adsorption behavior of modified steel slag on HEDP, and confirmed that the adsorption process was mainly completed by chemical precipitation and ligand exchange, which was a kind of chemical adsorption. The adsorption energy site analysis revealed the inhomogeneity of the energy distribution of the modified adsorption sites, which enhanced the affinity between the adsorbent and the adsorbate.
4. Regeneration performance and cyclic stability: The regeneration experiments of the adsorbent showed that the modified steel slag maintained a high regeneration capacity despite the decrease in adsorption efficiency after several cycles, and its performance was significantly better than that of the unmodified sample, demonstrating good cyclic stability and regeneration potential.
5. Microscopic characterization and elemental analysis: The SEM-EDS technique revealed significant changes in the surface morphology and elemental composition of the steel slag before and after adsorption, and the enrichment of phosphorus, carbon, oxygen, silicon, calcium, and other elements verified the validity of the adsorption process, and at the same time provided microscopic evidence of the adsorption mechanism.

In summary, HTS, as an efficient and environmentally friendly adsorbent, not only demonstrated excellent performance in removing HEDP, but also showed significant advantages in regeneration and cyclic stability, which provided a sustainable solution in the field of industrial wastewater treatment. Future studies could further explore the optimization of the modification conditions and the performance evaluation in different application scenarios to promote the wide application of modified steel slag in the field of wastewater treatment.

Author Contributions: Conceptualization, W.W. and Y.N.; methodology, Y.N.; software, Y.N. and Z.W.; validation, T.H.; formal analysis, X.X.; investigation, T.H.; resources, H.L. and P.L.; data curation, Y.N.; writing—original draft preparation, W.W. and Y.N.; writing—review and editing, B.W.; visualization, B.W.; supervision, B.W.; project administration, T.H.; funding acquisition, T.H. and B.W. All authors have read and agreed to the published version of the manuscript.

Funding: This work was supported by the National Natural Science Foundation of China (Nos. 21906078 provided by B.W., 52070137 provided by T.H.), Gusu Innovation and Entrepreneurship Leading Talent Plan (No. ZXL2022500).

Data Availability Statement: Data is contained within the article. The data is in figures and tables for the main text.

Acknowledgments: We thank Jingjing Yang for her help in data analysis.

Conflicts of Interest: Author Hanhan Liu was employed by the company Suzhou Chuanghailian Municipal Design Co. Author Peirong Li was employed by the company Suzhou Nadaqing Eco-Technology Co. The remaining authors declare that the research was conducted in the absence of any commercial or financial relationships that could be construed as a potential conflict of interest.

References

1. Rott, E.; Happel, O.; Armbruster, D.; Minke, R. Behavior of PBTC, HEDP, and Aminophosphonates in the Process of Wastewater Treatment. *Water* **2020**, *12*, 53. [CrossRef]
2. Wang, S.; Zhang, B.; Shan, C.; Yan, X.; Chen, H.; Pan, B. Occurrence and transformation of phosphonates in textile dyeing wastewater along full-scale combined treatment processes. *Water Res.* **2020**, *184*, 116173. [CrossRef] [PubMed]
3. Rott, E.; Steinmetz, H.; Metzger, J.W. Organophosphonates: A review on environmental relevance, biodegradability and re-moval in wastewater treatment plants. *Sci. Total Environ.* **2018**, *615*, 1176–1191. [CrossRef]
4. Lin, H.; Wang, Y.; Dong, Y. A review of methods, influencing factors and mechanisms for phosphorus recovery from sewage and sludge from municipal wastewater treatment plants. *J. Environ. Chem. Eng.* **2024**, *12*, 111657. [CrossRef]
5. Melia, P.M.; Cundy, A.B.; Sohi, S.P.; Hooda, P.S.; Busquets, R. Trends in the recovery of phosphorus in bioavailable forms from wastewater. *Chemosphere* **2017**, *186*, 381–395. [CrossRef] [PubMed]
6. Zeng, C.; Hu, H.; Wang, C.; Shi, Q.; Zhang, Q.; Chen, M.; Wang, Q.; Zhang, T. New insight into the changes in met-al-phosphonate complexes from the addition of CaCO3 to enhance ferric flocculation for efficient phosphonate removal. *Chemosphere* **2023**, *311*, 137078. [CrossRef]
7. Wu, B.; Wan, J.; Zhang, Y.; Pan, B.; Lo, I.M.C. Selective Phosphate Removal from Water and Wastewater using Sorption: Process Fundamentals and Removal Mechanisms. *Environ. Sci. Technol.* **2020**, *54*, 50–66. [CrossRef]
8. Zhang, Y.; Cao, H.; Lu, J.; Li, Y.; Bao, M. Enhanced photocatalytic activity of glyphosate over a combination strategy of GQDs/TNAs heterojunction composites. *J. Colloid Interface Sci.* **2022**, *607*, 607–620. [CrossRef]
9. Sahu, J.N.; Kapelyushin, Y.; Mishra, D.P.; Ghosh, P.; Sahoo, B.K.; Trofimov, E.; Meikap, B.C. Utilization of ferrous slags as coagulants, filters, adsorbents, neutralizers/stabilizers, catalysts, additives, and bed materials for water and wastewater treatment: A review. *Chemosphere* **2023**, *325*, 138201. [CrossRef]
10. Claveau-Mallet, D.; Boutet, E.; Comeau, Y. Steel slag filter design criteria for phosphorus removal from wastewater in de-centralized applications. *Water Res.* **2018**, *143*, 28–37. [CrossRef]
11. Cha, W.; Kim, J.; Choi, H. Evaluation of steel slag for organic and inorganic removals in soil aquifer treatment. *Water Res.* **2006**, *40*, 1034–1042. [CrossRef] [PubMed]
12. Wang, K.; Qian, C.; Wang, R. The properties and mechanism of microbial mineralized steel slag bricks. *Constr. Build. Mater.* **2016**, *113*, 815–823. [CrossRef]
13. Shi, C.; Wang, X.; Zhou, S.; Zuo, X.; Wang, C. Mechanism, application, influencing factors and environmental benefit as-sesment of steel slag in removing pollutants from water: A review. *J. Water Process Eng.* **2022**, *47*, 102666. [CrossRef]
14. Lu, H.; Xiao, L.; Wang, T.; Lu, S.; Wang, H.; Guo, X.; Li, J. The application of steel slag in a multistage pond constructed wetland to purify low-phosphorus polluted river water. *J. Environ. Manag.* **2021**, *292*, 112578. [CrossRef] [PubMed]
15. Yang, L.; Wen, T.; Wang, L.; Miki, T.; Bai, H.; Lu, X.; Yu, H.; Nagasaka, T. The stability of the compounds formed in the process of removal Pb(II), Cu (II) and Cd(II) by steelmaking slag in an acidic aqueous solution. *J. Environ. Manag.* **2019**, *231*, 41–48. [CrossRef] [PubMed]
16. Zhang, Z.; Feng, Y.; Liu, N.; Zhao, Y.; Wang, X.; Yang, S.; Long, Y.; Qiu, L. Preparation of Sn/Mn loaded steel slag zeolite particle electrode and its removal effect on rhodamine B(RhB). *J. Water Process. Eng.* **2020**, *37*, 101417. [CrossRef]
17. Shao, Q.; Yi, Y.; Xie, Y.; Yang, H.; Guo, J.; Liu, Z.; Chen, Y.; Wan, J. Selective sorption of organic phosphonate HEDP by steel slag: Efficiency and mechanism. *Process. Saf. Environ. Prot.* **2024**, *186*, 645–655. [CrossRef]
18. *GB 5085.6-2007*; Identification Standards for Hazardous Wastes Identification for Toxic Substance Content. China Environmental Science Press: Beijing, China, 2017.
19. Wang, S.; Yao, S.; Du, K.; Yuan, R.; Chen, H.; Wang, F.; Zhou, B. The mechanisms of conventional pollutants adsorption by modified granular steel slag. *Environ. Eng. Res.* **2021**, *26*, 190352. [CrossRef]
20. Okoye, P.U.; Abdullah, A.Z.; Hameed, B.H. Stabilized ladle furnace steel slag for glycerol carbonate synthesis via glycerol transesterification reaction with dimethyl carbonate. *Energy Conv. Manag.* **2017**, *133*, 477–485. [CrossRef]
21. Gagliano, E.; Falciglia, P.P.; Zaker, Y.; Karanfil, T.; Roccaro, P. Microwave regeneration of granular activated carbon saturated with PFAS. *Water Res.* **2021**, *198*, 117121. [CrossRef]
22. Nahm, S.W.; Shim, W.G.; Park, Y.-K.; Kim, S.C. Thermal and chemical regeneration of spent activated carbon and its adsorption property for toluene. *Chem. Eng. J.* **2012**, *210*, 500–509. [CrossRef]
23. Vanvliet, B.; Venter, L. Infrared Thermal Regeneration of Spent Activated Carbon from Water Reclamation. *Water Sci. Technol.* **1985**, *17*, 1029–1042. [CrossRef]
24. Sun, S.; Shan, C.; Yang, Z.; Wang, S.; Pan, B. Self-Enhanced Selective Oxidation of Phosphonate into Phosphate by Cu(II)/H_2O_2: Performance, Mechanism, and Validation. *Environ. Sci. Technol.* **2022**, *56*, 634–641. [CrossRef] [PubMed]
25. Wang, S.; Sun, S.; Shan, C.; Pan, B. Analysis of trace phosphonates in authentic water samples by pre-methylation and LC-Orbitrap MS/MS. *Water Res.* **2019**, *161*, 78–88. [CrossRef] [PubMed]

26. Du, W.; Li, Y.; Xu, X.; Shang, Y.; Gao, B.; Yue, Q. Selective removal of phosphate by dual Zr and La hydroxide/cellulose-based bio-composites. *J. Colloid Interface Sci.* **2019**, *533*, 692–699. [CrossRef] [PubMed]
27. Cao, L.; Shen, W.; Huang, J.; Yang, Y.; Zhang, D.; Huang, X.; Lv, Z.; Ji, X. Process to utilize crushed steel slag in cement industry directly: Multi-phased clinker sintering technology. *J. Clean Prod.* **2019**, *217*, 520–529. [CrossRef]
28. Gonzalez, P.L.L.; Novais, R.M.; Labrincha, J.A.; Blanpain, B.; Pontikes, Y. Modifications of basic-oxygen-furnace slag microstructure and their effect on the rheology and the strength of alkali-activated binders. *Cem. Concr. Compos.* **2019**, *97*, 143–153. [CrossRef]
29. Yu, J.; Liang, W.; Wang, L.; Li, F.; Zou, Y.; Wang, H. Phosphate removal from domestic wastewater using thermally modified steel slag. *J. Environ. Sci.* **2015**, *31*, 81–88. [CrossRef]
30. Rasee, A.I.; Awual, E.; Rehan, A.I.; Hossain, M.S.; Waliullah, R.M.; Kubra, K.T.; Sheikh, M.C.; Salman, M.S.; Hasan, M.N.; Hasan, M.M.; et al. Efficient separation, adsorption, and recovery of Samarium(III) ions using novel ligand-based composite adsorbent. *Surf. Interfaces* **2023**, *41*, 103276. [CrossRef]
31. Bulyarskii, S.V.; Basaev, A.S. Thermodynamics and kinetics of adsorption of atoms and molecules by carbon nanotubes. *J. Exp. Theor. Phys.* **2009**, *108*, 688–698. [CrossRef]
32. Zhou, Z.; Xu, Q.; Wu, Z.; Fang, X.; Zhong, Q.; Yang, J.; Yan, J.; Li, Q. Preparation and characterization of clay-oyster shell composite adsorption material and its application in phosphorus removal from wastewater. *Sustain. Chem. Pharm.* **2023**, *32*, 101023. [CrossRef]
33. Li, X.; Wen, B.; Li, Y. Adsorption of the Malachite Green by Magnetic Clam Shell Powder. *Pol. J. Environ. Stud.* **2021**, *30*, 717–726. [CrossRef] [PubMed]
34. Li, C.; Yang, Q.; Liu, D.; Nie, H.; Liu, Y. Removal of organic phosphonate HEDP by Eu-MOF/GO composite membrane. *J. Environ. Chem. Eng.* **2021**, *9*, 106895. [CrossRef]
35. Li, C.; Yang, Q.; Nie, H.; Liu, D.; Liu, Y. Adsorption removal of organic phosphonate HEDP by magnetic composite doped with different rare earth elements. *Chem. Eng. J. Adv.* **2022**, *9*, 100221. [CrossRef]
36. Jiang, H.; Li, Q.; Sun, J.; Huang, Y.; Zhang, P.; Mao, Y.; Qu, Y.; Liu, X. Studies on competitive adsorption characteristics of bisphenol A and 17α-ethinylestradiol on thermoplastic polyurethane by site energy distribution theory. *Environ. Geochem. Health* **2023**, *45*, 5181–5194. [CrossRef] [PubMed]
37. Alhujaily, A.; Mao, Y.; Zhang, J.; Ifthikar, J.; Zhang, X.; Ma, F. Facile fabrication of Mg-Fe-biochar adsorbent derived from spent mushroom waste for phosphate removal. *J. Taiwan Inst. Chem. Eng.* **2020**, *117*, 75–85. [CrossRef]
38. Li, C.; Yang, Q.; Lu, S.; Liu, Y. Adsorption and mechanism study for phosphonate antiscalant HEDP removal from reverse osmosis concentrates by magnetic La/Zn/Fe_3O_4@PAC composite. *Colloids Surf. A Physicochem. Eng. Asp.* **2021**, *613*, 126056. [CrossRef]
39. Liu, X.; Tian, J.; Li, Y.; Sun, N.; Mi, S.; Xie, Y.; Chen, Z. Enhanced dyes adsorption from wastewater via Fe_3O_4 nanoparticles functionalized activated carbon. *J. Hazard. Mater.* **2019**, *373*, 397–407. [CrossRef] [PubMed]
40. Peng, Y.; Azeem, M.; Li, R.; Xing, L.; Li, Y.; Zhang, Y.; Guo, Z.; Wang, Q.; Ngo, H.H.; Qu, G.; et al. Zirconium hydroxide nanoparticle encapsulated magnetic biochar composite derived from rice residue: Application for As(III) and As(V) polluted water purification. *J. Hazard. Mater.* **2022**, *423*, 127081. [CrossRef]
41. Wu, B.; Fang, L.; Fortner, J.D.; Guan, X.; Lo, I.M.C. Highly efficient and selective phosphate removal from wastewater by magnetically recoverable La(OH)3/Fe_3O_4 nanocomposites. *Water Res.* **2017**, *126*, 179–188. [CrossRef]